



46TH TURBOMACHINERY & 33RD PUMP SYMPOSIA
HOUSTON, TEXAS | DECEMBER 11-14, 2017
GEORGE R. BROWN CONVENTION CENTER

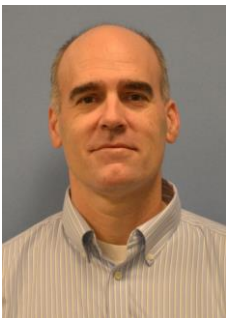
Challenges with a large high pressure water injection pump

Ed Wilcox

Consulting Machinery Engineer
Chevron Energy Technology Company
Houston, TX

Martin Uere Villoria

Global Head of Advanced Engineering Power Generation
Sulzer, Inc
Winterthur, Switzerland



Ed Wilcox is a Consulting Machinery Engineer with the Energy Technology Company (ETC) of Chevron. Prior to this he worked for Conoco and Lyondell Chemical as a machinery engineer. He has a BSME degree from the University of Missouri-Rolla and an MSME degree from Oklahoma State University. He is a Vibration Institute Category IV Vibration Specialist and a registered Professional Engineer in the State of Oklahoma. Mr. Wilcox has authored multiple papers in the areas of rotordynamics, vibration analysis, and performance testing at both the Texas A&M Turbomachinery and Pump Symposia, along with several magazine articles.



Martin Uere Villoria is the Global Head of Advance Engineering Power Generation at Sulzer. He has worked within the Pumps Equipment division since 2008 in Switzerland, Brazil, and the UK. During this time, he has been responsible for pump development projects in upstream oil and gas, with water injection systems and seawater lift pumps. Beforehand, he worked in the German Navy as operational officer and studied mechanical engineering with a focus on turbomachinery. Mr. Uere Villoria authored several Sulzer papers as well as a paper about an optimization of Boiler Feed Multistage pumps for the VDMA (German Mechanical Engineering Industry Association).

ABSTRACT

In 2009, a project was initiated to install two large high pressure water injection pumps producing 586 bar (8500 psig) discharge at 9.3MW (12,500 hp) on an existing deep water offshore platform. Several technical challenges were overcome during the factory acceptance testing of the pumps that led to some seemingly minor design changes. After installation and commissioning, the pumps have operated with a mixture of both good reliability and sudden failures. The paper will detail the pulsation testing



that was completed during the FAT of the pump and how the pulsation levels were evaluated and addressed. An in-depth look at a total shaft failure, its causes, and the design changes taken to address it are provided in detail. Additionally, the analysis of a second pulsation related failure will be reviewed to examine some rather unique effects not seen before by the OEM or operator.

BACKGROUND

A project was initiated to add water injection in 2009 to a deep water platform in the Gulf of Mexico to increase crude production. The basic process conditions are specified in Table 1. Because of power limitations on the platform, a turbine driver was selected in the configuration shown in Figure 1. At the time, several previous projects in the Gulf of Mexico had been completed that were similar in process conditions, but only one other was equal in rated discharge pressure (Thunderhorse), see Figure 2. The Thunderhorse pumps had undergone a rigorous qualification and testing process, but had very limited operation experience at the time [1]. Similar water injection applications on the Atlantis and Holstein platforms had been running for a short period at the time of the qualification of the subject pump. Because of this and the turbine driver, a technical qualification was undertaken to ensure that the pump would be able to reliably meet the required process conditions.

Parameter	Rated	Fracturing (max)
Head m (ft)	4877 (16,000)	5688 (18661)
Differential Pressure bard (psid)	487 (7065)	568 (8240)
Flow m3/h (USGPM)	334 (1470)	Minimum
Temperature deg. C (F) Max/Norm	43 to 66 (110 to 150)	
Speed (rpm)	5571	5948
Specific gravity	1.02	1.02

Table 1. Water injection specifications

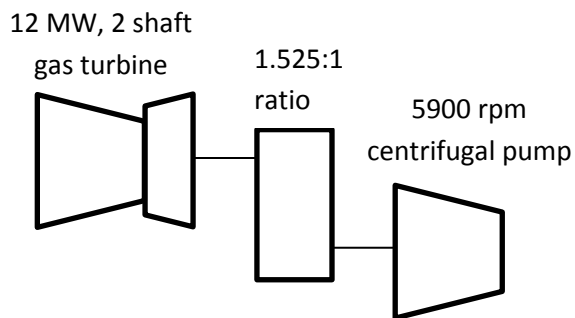


Figure 1. Water injection train configuration

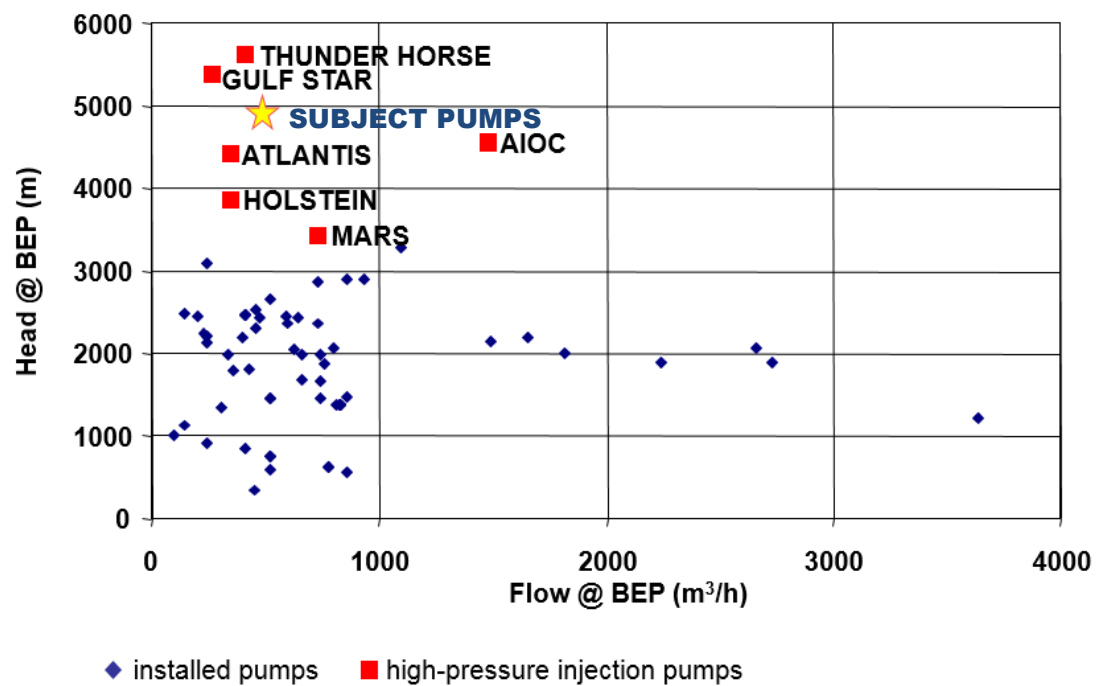


Figure 2. Previous water injection experience(Sulzer)

Due to the high differential pressure required at relatively low flow, 12 stages were needed even at nearly 6000 rpm. The pump selected was a back to back configuration, see Figure 3. This configuration incorporates center and throttle bushings which produced a Lomakin bearing at each location, thus adding rotor support even with worn clearances. The reference pump (Thunder Horse) which represents the same rotor configuration was subjected to a 200% clearance test and had shown acceptable



vibration levels proving that for this duty the configuration was a rotordynamically suitable selection. A basic listing of the pump mechanical design details are shown in Table 2.

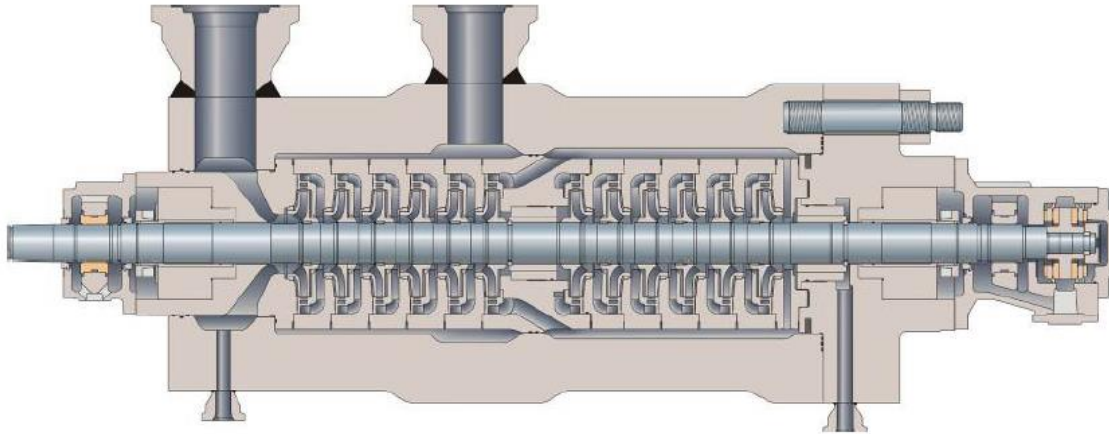
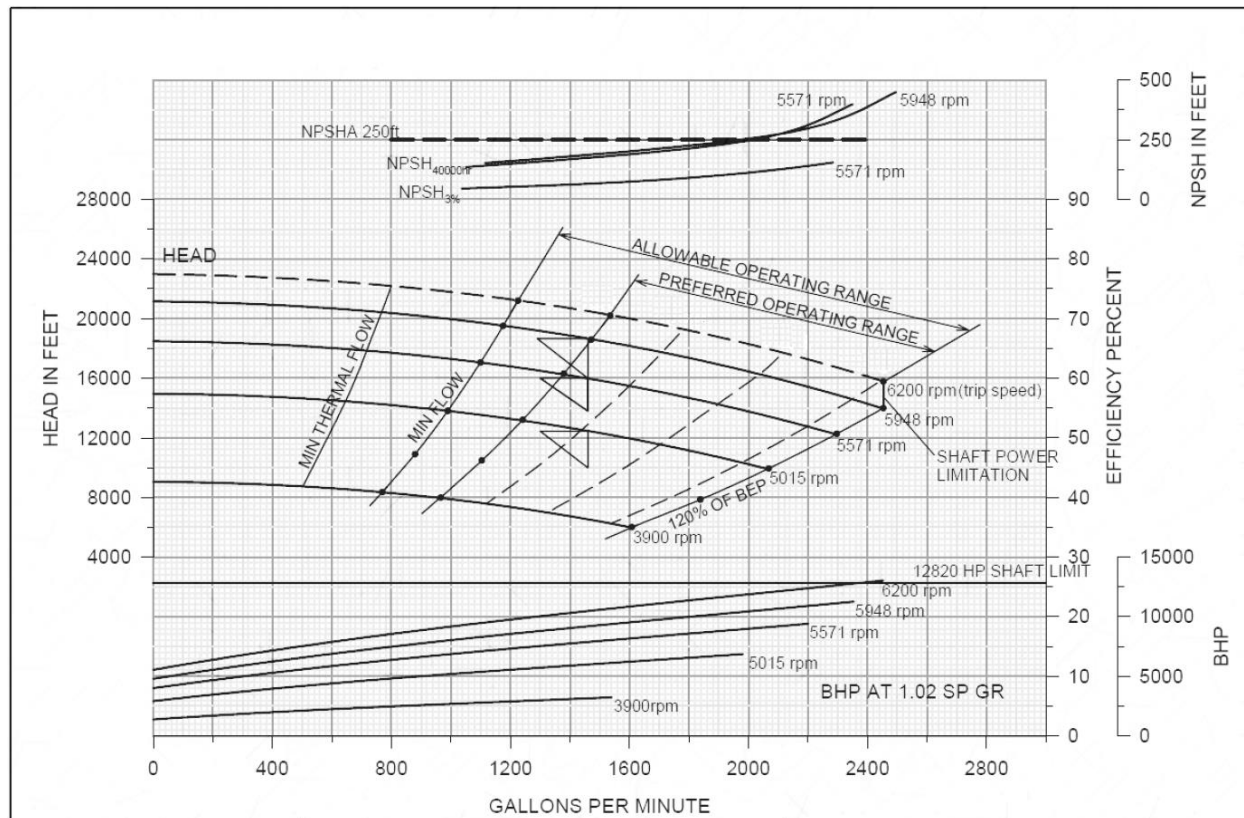


Figure 3. Back-to-back high pressure barrel design(Sulzer)

# of stages	12
Impeller diameter	288 mm (11.3")
Material of construction	API D-2 (A276 super duplex)
Operating speed range	5015-5948 rpm
Stationary component design	Diffuser/radial split, double casing (stage case & barrel)
Radial bearing	Hydrodynamic, cylindrical lobed bearing
Thrust bearing	Hydrodynamic tilting pad, self-equalizing
Seal	Dual pressurized, API plan 53

Table 2. Mechanical design details

The pump selection was based on prior qualification and experience of the larger Thunderhorse pump (appx 70 MBPD) rather than the actual design flow of 50 MBPD because the hydraulic design of the Thunderhorse pump had been thoroughly qualified and tested. This resulted in the pump selection being on the far left side of the preferred operating range, see Figure 4. The project team considered it to be more of a risk to select a scaled (but unproven) hydraulic design, rather than a proven design that was on the edge of its preferred operating range.



NOTE: Shaft power limit is set using normal shaft service factor of approximately 8

Figure 4. Performance curve(Sulzer)

Because of the operating point and due to impeller failures on similar pump types in the time between the original pump design and the present risk study, one of the major concerns from the qualification was potential for vane pass pulsation that could lead to impeller failure. To address these concerns, a qualification plan was developed that included the following:

- Impeller fatigue analyses based on the latest findings of recent RCFA's [2], [3]
- Re-visiting the design report of the original pump considering the new duty
- Natural frequency prediction and testing of the pump impellers
- Full load string test with the gas turbine driver
- Measurement of pressure pulsation during the string test



46TH **TURBOMACHINERY** & 33RD **PUMP SYMPOSIA**
HOUSTON, TEXAS | DECEMBER 11-14, 2017
GEORGE R. BROWN CONVENTION CENTER

ANALYTICAL ANALYSIS

As part of the technical qualification plan, all relevant design reports which had been created during this pump size original design phase [1] had been reviewed again considering the new duty. Actions had been compiled to a Risk Mitigation Plan and had been built into the engineering schedule prior to releasing all components to manufacturing. The bolting material had changed due to unavailability in the supply chain thus, the pressure boundary analysis was re-visited.

Figure 5 is a graphical illustration of several of the different impeller mode shapes as predicted by FEA analysis. The modes were calculated and measured in air and water, see Table 3. As would be expected the wetted modes are calculated to be much lower in frequency. Experimental verification of the wetted modes did not produce consistent results. The wetted natural frequencies are a strong function of the volume of water surrounding the impeller. Since the correct clearance/volume of water around the impeller only exists inside the pump, the wetted modes were not verified.

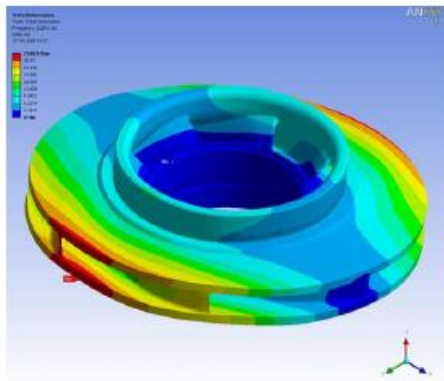


Figure B-1: Rocking Mode

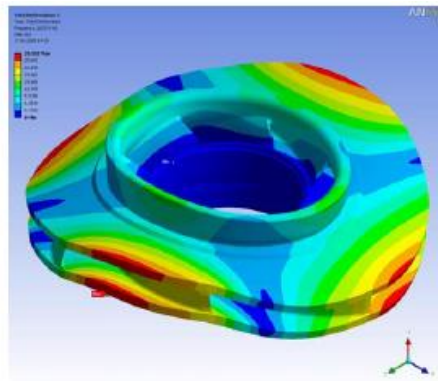


Figure B-2: 2-Diameter Mode

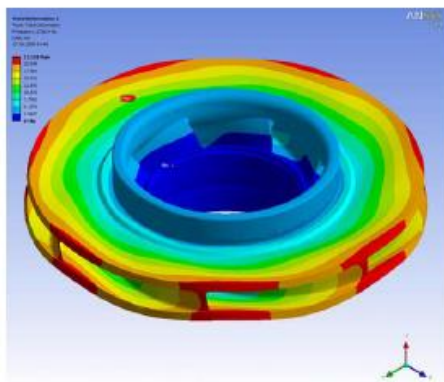


Figure B-3: Umbrella Mode

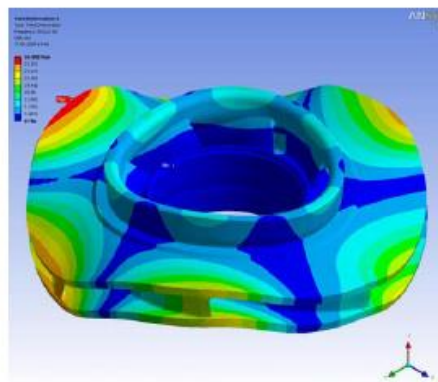


Figure B-4: 3-Diameter Mode

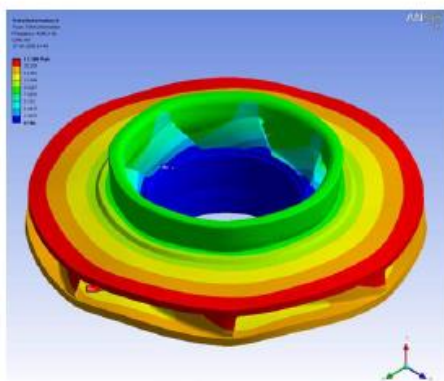


Figure B-5: Torsional Mode

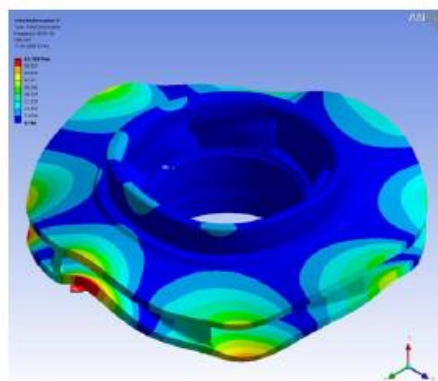


Figure B-6: 4-Diameter Mode

Figure 5a. Illustrations of various FEA calculated impeller modes(Sulzer)



Method	Rocking	Umbrella	2-Diameter	3-Diameter
Calculated (air)	2335	2707	2676	3912
Measured(air)	1724	2816	2460	—
Calculated(water)	1095	1110	1486	2449

Table 3. Comparison of Sulzer calculated and measured impeller modes (hz)

Due to previous root cause failure analyses on water injection pump impeller failures, the natural frequency excitation of the impellers had been excluded as a potential physical cause of failure. The dynamic forces from pressure pulsations and rotating stall phenomena and resulting high cycle stresses in high stress concentration areas of the impeller outlet were identified as the primary cause of impeller failure [1]. As previously mentioned, the duty for the subject pump required considerable operation at part load (see Figure 4). The impeller was designed to minimize the pressure pulsations which occur in part load operation of high energy pumps. Also, the impeller design was evaluated in a way to maximize the fatigue resistance of the high stress areas using FEA methods [3]. The pressure pulsation data measured from impellers with similar hydraulics was used to simulate the occurring loads and assess the safety factor against fatigue failure for an unlimited number of cycles.

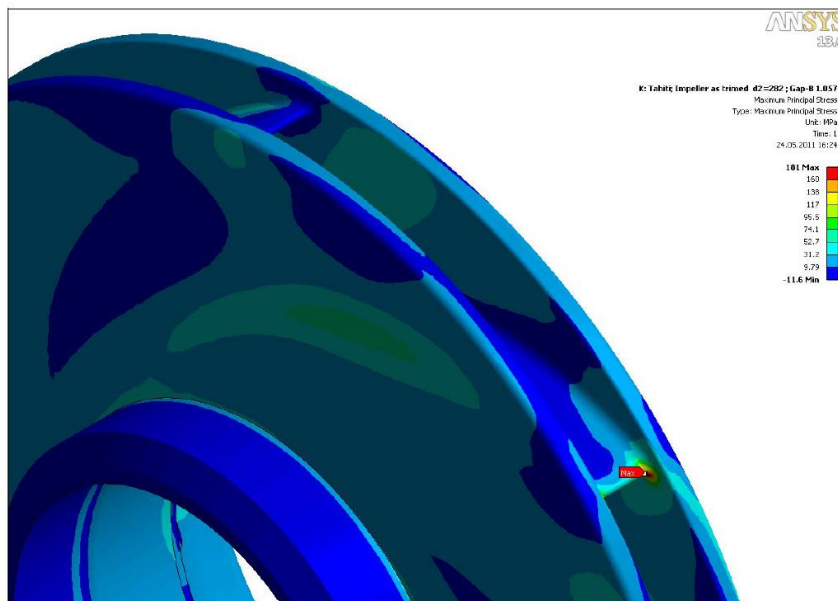


Figure 5b. Illustrations of various FEA calculated impeller stresses(Sulzer)



Figure 5b shows the evaluated stresses at the impeller outlet where typical failures had occurred on previous pumps using scaled pressure amplitudes from previous investigations and tests. The hydraulic and mechanical design of the impellers were qualified for steady state, reliable operation along the allowable operating range for an unlimited number of pressure peak cycles and rotating stall. These conditions are unavoidable for centrifugal pump radial impellers running outside their best efficiency window.

FULL LOAD TEST

Figures 6 and 7 show pictures of the overall string test set-up as well as the instrumentation used to measure the dynamic pressure during the full-load string test. The dynamic pressure was recorded at three different locations (suction, 1st stage outlet, and discharge) during the test. The results of the testing are shown in Table 4 and Figure 8 below. As expected, the pulsation is a strong function of speed and proximity to minimum flow. The overall pulsation levels were relatively low, with a maximum dynamic pressure recording of 1.66 bar (24 psi) at maximum speed and minimum flow. Additionally, a spectrum of one of the dynamic pressure points is shown in Figure 9. Of concern is the peak on the 1st stage impeller discharge spectrum at approximately 1400 hz. This is relatively close to the 2-Diameter mode shown in Table 3. Likewise, because all of the impellers have 7 vanes, this is relatively close to the 2nd harmonic of vane pass frequency ($6000 \text{ rpm} / 60 \times 7 \text{ vanes} \times 2 = 1400 \text{ hz}$).



Figure 6. Water injection train during mechanical string test(Sulzer)



46TH TURBOMACHINERY & 33RD PUMP SYMPOSIA
HOUSTON, TEXAS | DECEMBER 11-14, 2017
GEORGE R. BROWN CONVENTION CENTER

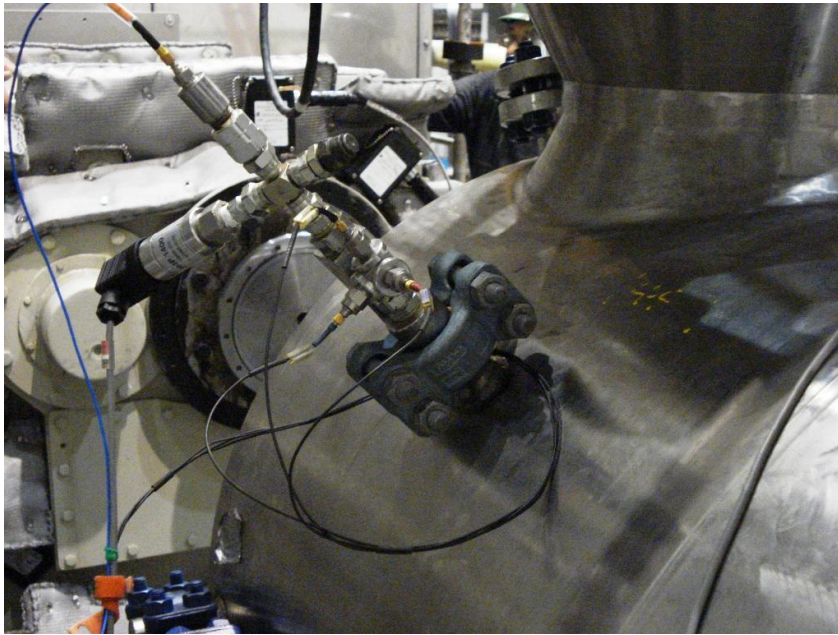


Figure 7. Dynamic pressure transducer on 1st stage impeller discharge tap during string test(Sulzer)



Point	Time	Speed	Flow	Pump INLET			1st STAGE outlet			Pump OUTLET		
				mean M bar	dynamic D bar (rms) (5 Hz - 10kHz)	D/M %	mean M bar	dynamic D bar (rms) (5 Hz - 10kHz)	D/M %	mean M bar	dynamic D bar (rms) (5 Hz - 10kHz)	D/M %
1	14:48	5950	172	5.30	0.32	6.0	52.5	1.66	3.2	609	0.80	0.13
2	14:51	5950	277	5.20	0.16	3.1	52.9	1.12	2.1	596	0.54	0.09
3	14:55	5950	332	5.80	0.13	2.3	51.4	1.04	2.0	580	0.53	0.09
4	15:02	5950	459	5.74	0.13	2.3	44.6	0.71	1.6	511	0.45	0.09
5	15:16	5950	508	6.01	0.14	2.3	42.3	0.66	1.6	483	0.43	0.09
6	15:11	5950	553	5.97	0.14	2.4	39.3	0.59	1.5	450	0.46	0.10
7	15:32	5571	161	6.33	0.42	6.6	47.8	1.62	3.4	543	1.13	0.21
8	15:36	5571	259	6.33	0.15	2.3	48.3	0.87	1.8	525	0.47	0.09
9	15:41	5571	331	6.25	0.09	1.4	45.4	0.48	1.1	502	0.42	0.08
10	15:45	5571	430	6.12	0.09	1.4	39.8	0.58	1.4	449	0.40	0.09
11	15:48	5571	476	6.05	0.09	1.5	37.9	0.54	1.4	424	0.41	0.10
12	15:54	5571	518	5.98	0.11	1.8	35.1	0.46	1.3	394	0.41	0.10
13	16:11	5015	145	6.44	0.30	4.6	40.2	1.13	2.8	442	0.74	0.17
14	16:14	5015	233	6.36	0.13	2.0	40.6	0.56	1.4	429	0.36	0.08
15	16:17	5015	332	6.25	0.10	1.5	36.7	0.39	1.1	394	0.33	0.08
16	16:19	5015	387	6.19	0.10	1.7	34.3	0.39	1.1	369	0.34	0.09
17	16:20	5015	428	6.12	0.10	1.7	32.2	0.41	1.3	346	0.35	0.10
18	16:22	5015	466	6.07	0.11	1.8	30.0	0.41	1.4	323	0.37	0.11
10% speed increments	18:30	3900	173	6.47	0.10	1.5	27.4	0.42	1.5	267	0.29	0.11
	18:35	4293	195	6.45	0.10	1.6	31.6	0.46	1.5	319	0.32	0.10
	18:38	4692	220	6.43	0.11	1.7	36.5	0.45	1.2	377	0.33	0.09
	18:43	5067	244	6.44	0.11	1.7	41.1	0.46	1.1	435	0.35	0.08
	18:47	5476	274	6.41	0.13	2.0	45.7	0.60	1.3	503	0.43	0.09
	18:50	5850	304	6.38	0.14	2.1	50.7	0.93	1.8	569	0.49	0.09
	18:52	5950	326	6.36	0.13	2.0	51.5	0.97	1.9	583	0.53	0.09
	18:54	5950	332	6.36	0.12	1.9	51.5	0.96	1.9	582	0.52	0.09
Mech. run	21:42	5950	332	6.43	0.12	1.9	52.1	1.21	2.3	581	0.53	0.09

Table 4. Pressure pulsation measurements during string test (Sulzer)

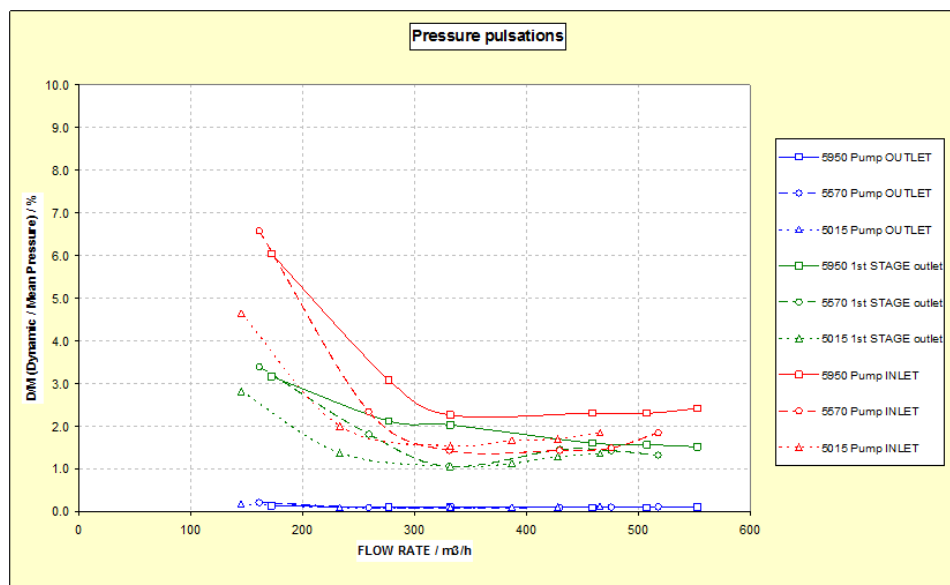


Figure 8. Pressure pulsation/mean pressure versus flow (Sulzer)

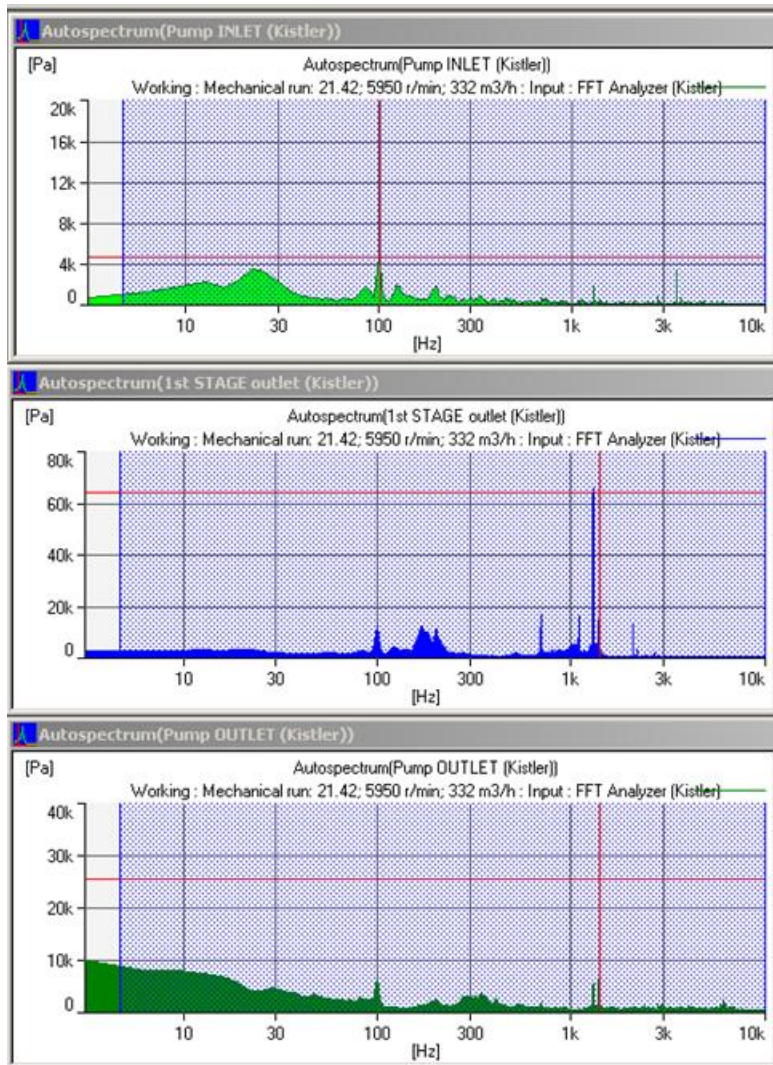


Figure 9. Spectrum of pressure pulsation at inlet (top), 1st stage outlet (middle), and pump outlet (lower) (Sulzer) 10000 Pa = 0.1 Bar = 1.45 psi



MODIFICATIONS

While the pulsation levels didn't appear to be high, there was concern over the pulsation peak that was close to the 2-D impeller mode. The Industry experience has shown that increasing the clearance between the impeller vane outside diameter and the diffuser vane inside diameter (commonly called the B gap) decreases the pulsation levels. Figure 10 is an illustration showing the basic pump impeller geometry at the outlet. Equation 1 from Gulich [1] roughly indicates the relationship between pulsation generated from high energy centrifugal pumps and the B gap. This equation shows that if the B gap is doubled, the pulsation is reduced by approximately 40% with the downside of losing efficiency due to increased volumetric losses. For the subject pump, if the impeller/diffuser gap ratio was doubled from 3.5 to 7.0% the OEM calculated impeller fatigue design factor increases to 1.54. However, the 7% B gap resulted in too large reduction in the produced head for the water injection system. According to the OEM and based on the previously stated impeller fatigue analyses, a B gap of 5.7% was required to meet the latest internal design criteria of 1.3. This should improve the impellers reliability because the pulsation energy is predicted to be reduced by approximately 30%.

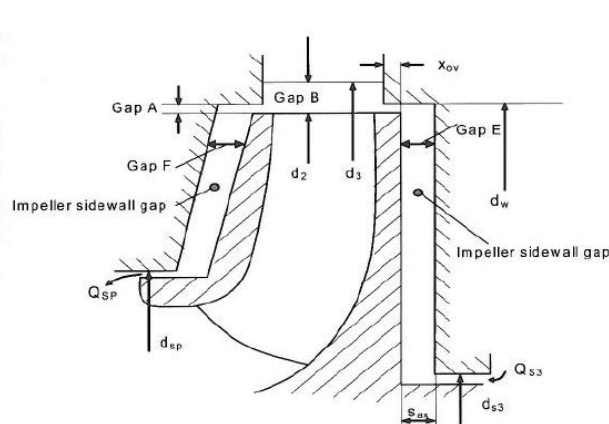


Figure 10. Centrifugal pump impeller/diffuser cross-section showing impeller/diffuser gap ratio (d_3/d_2), commonly called "B" gap



$$pulsation \propto \left(\frac{d_3}{d_2} - 1 \right)^{-0.77} \quad (1)$$

An additional spare cartridge was purchased with 285 mm impellers, instead of the original 288 mm (this increased the B-gap from 3.5 to 5.7%). Performance tests showed that this reduced the measured pulsation over most of the flow range, see Figure 11, but it also reduced the produced head by approximately 8% which is more than the affinity laws predicted $(285/288)^2=0.979$, see Figure 12. To meet injection demands the maximum speed of the power turbine was increased from 9060 to 9453 rpm, resulting in a pump speed of 5940 to 6200 RPM for the 285 mm pump cartridge only. This was possible because the original design limited the gas turbine's power turbine speed to 95 % of Max Continuous Operating Speed.

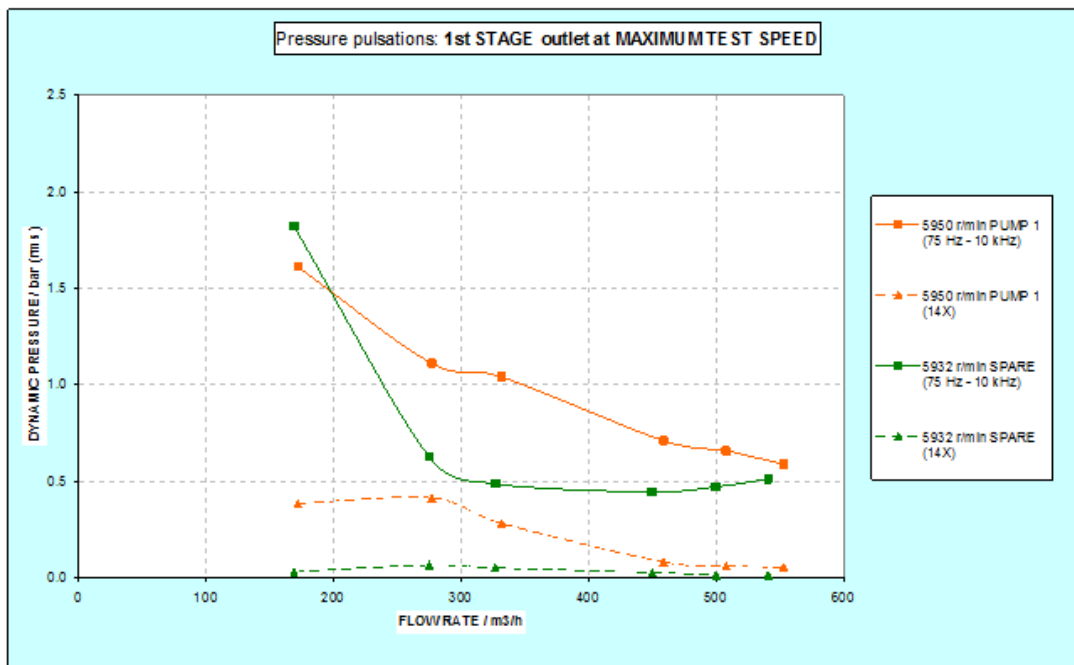


Figure 11. Comparison of 288 mm trim and 285 mm trim pulsation as % of line pressure (1st stage) 1 Bar = 14.5 psi



46TH TURBOMACHINERY & 33RD PUMP SYMPOSIA
HOUSTON, TEXAS | DECEMBER 11-14, 2017
GEORGE R. BROWN CONVENTION CENTER

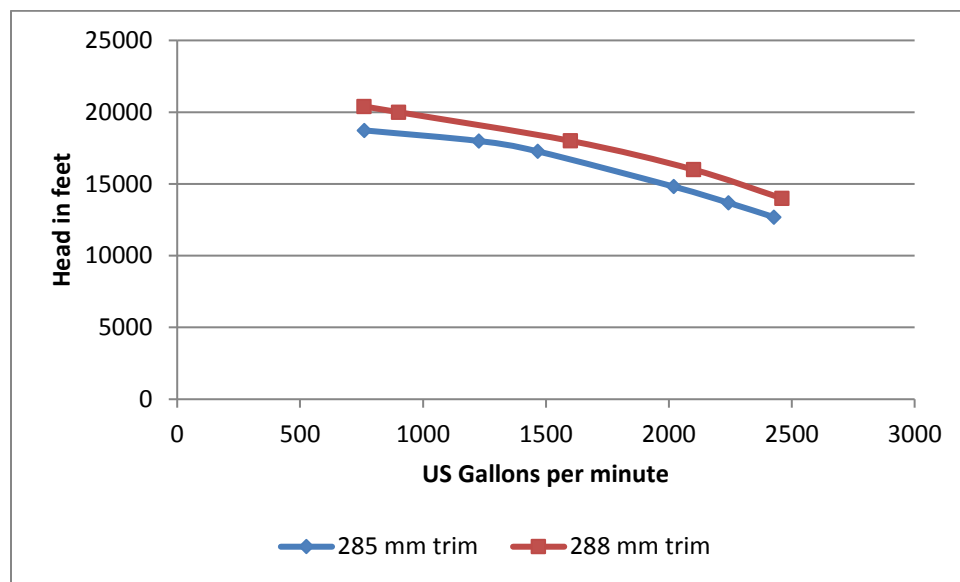


Figure 12. Comparison of head produced by 288 and 285 mm trim (5948 rpm)

OPERATION

The two pumps with 288 mm impellers were commissioned in 2012 and ran with no problems until on March 28, 2013, when a high vibration trip occurred on the outboard end of the B pump. A rather unique characteristic of the vibration was that the outboard radial vibration began dropping prior to the rapid increase at the trip, which also coincided with an erratic flow reading, see Figure 13. The pump was restarted but the required injection pressure could not be reached due to the continued high vibration on the outboard end of the pump.

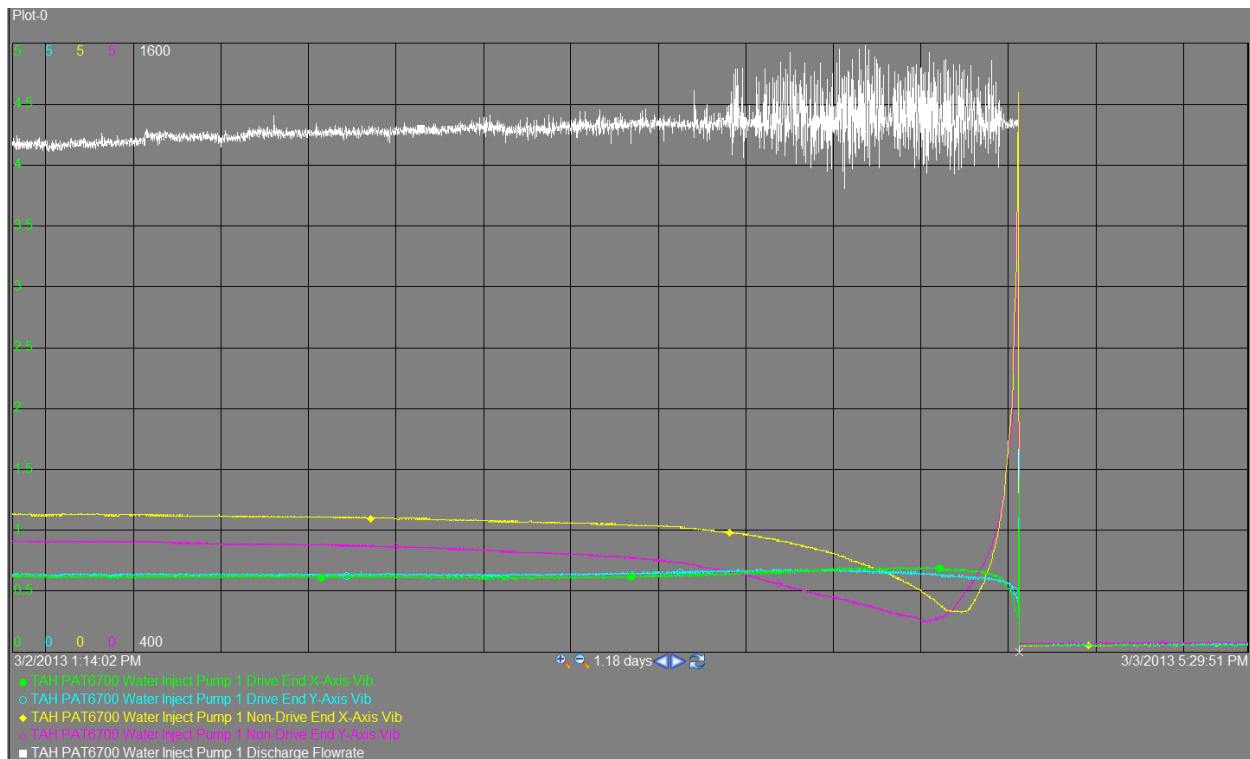


Figure 13. Trend of pump radial vibration (NDE-yellow, magenta), (DE radial-blue, green), flow - white

Teardown of the pump revealed that the shaft had failed completely underneath the throttle sleeve on the non-drive end at an O-ring groove in the shaft, see Figures 14 and 15. This was extremely unusual because the only power transmitted in that portion of the shaft is to drive the OB mechanical seal, OB sleeve bearing and thrust bearing (approximately 30 kW (40 hp)). Due to axial loads generated by the impellers and combination of torque loads, a back to back rotor experiences the highest loads at the center sleeve section (>100 times higher than at the failure location). As can be seen the failure is a torsional high cycle fatigue failure of the shaft that ended with ductile overload at the center (see Figures 16 and 17). Mechanical testing confirmed that the A276 super duplex shaft had poor fracture toughness at -40C and 70 C, see Tables 5 and 6. ASTM A276 does not specify acceptance criteria which are typically based upon specific purchaser requirements. A well heat treated super duplex forging should have good fracture toughness to low temperatures, and as such it is normal to conduct impact tests at -40°F (-40°C). Typical minimum acceptance criteria at this temperature are approximately 30 ft.lb (40J). Despite the low fracture toughness, the yield and ultimate stresses were still within ASTM



specification, while the elongation was slightly below specification. However, this was still acceptable in terms of OEM generic recommendations (min. 15% for high energy shafts).

The shaft forging was tested before it was machined and stress relieved, see Table 7. The significant decrease in Charpy values indicate that low temperature stress relief process performed after initial machining had significantly reduced the shaft's fracture toughness.

Although the O-ring groove had well profiled corners, the groove itself could still generate a localized stress concentration, which combined with the additional stiffness provided by the bushing makes this location more sensitive to cyclic loading. Due to the brittle nature of the shaft material at this location, minimal crack propagation would have been required before a sudden transgranular cleavage fracture caused complete shaft failure.

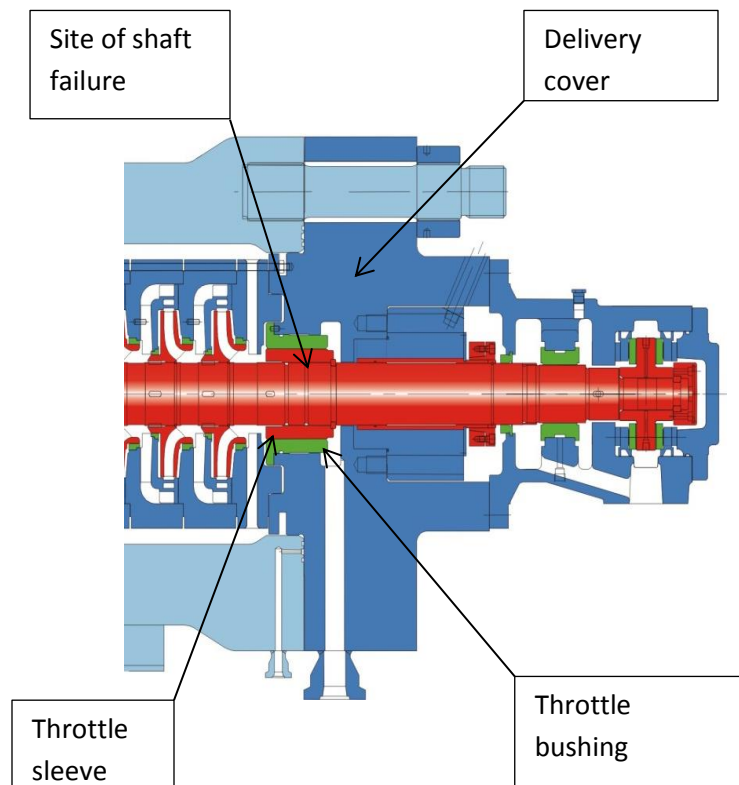


Figure 14. Cross-section of outboard (NDE) of water injection pump(Sulzer)



46TH TURBOMACHINERY & 33RD PUMP SYMPOSIA
HOUSTON, TEXAS | DECEMBER 11-14, 2017
GEORGE R. BROWN CONVENTION CENTER



Figure 15. Failed shaft sections (NDE on Left hand side). Note O-ring groove at failure point



46TH **TURBOMACHINERY** & 33RD **PUMP SYMPOSIA**
HOUSTON, TEXAS | DECEMBER 11-14, 2017
GEORGE R. BROWN CONVENTION CENTER

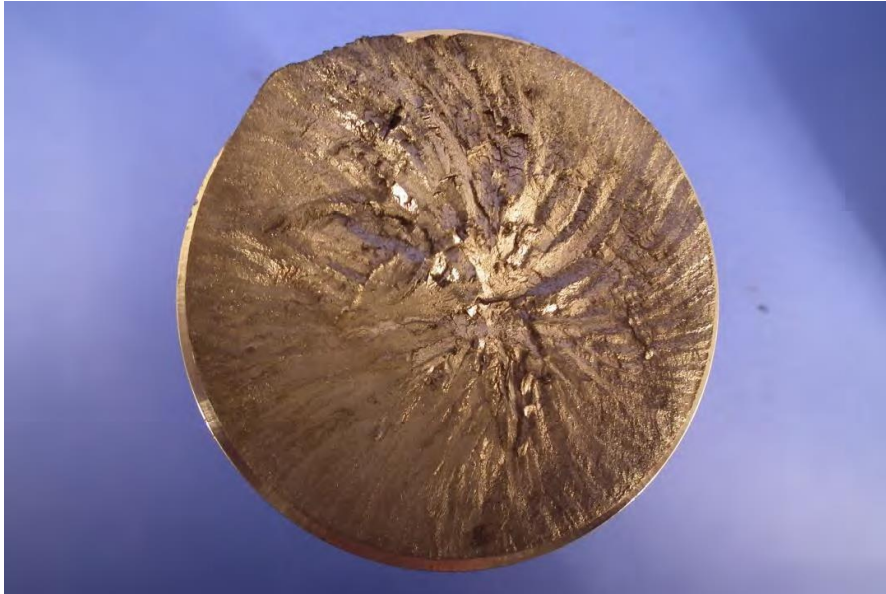


Figure 16. NDE (Non-Drive End) shaft fracture face



Figure 17. DE shaft fracture face



Location	Sample	Absorbed Energy ⁽¹⁾⁽²⁾	Shear	Lateral Expansion
0.25 Diameter	1	5ft.lb (6.8J)	5%	4mils (0.101mm)
	2	5ft.lb (6.8J)	5%	5mils (0.127mm)
	3	6ft.lb (8.1J)	5%	3mils (0.076mm)
0.5 Diameter	1	5ft.lb (6.8J)	5%	5mils (0.127mm)
	2	7ft.lb (9.5J)	5%	5mils (0.127mm)
	3	6ft.lb (8.1J)	5%	3mils (0.076mm)
0.75 Diameter	1	6ft.lb (8.1J)	5%	4mils (0.101mm)
	2	5ft.lb (6.8J)	5%	3mils (0.076mm)
	3	6ft.lb (8.1J)	5%	4mils (0.101mm)

Table 5. Failed shaft low temperature Charpy impact results

Location	Sample	Absorbed Energy ⁽¹⁾⁽²⁾	Shear	Lateral Expansion
0.25 Diameter (Longitudinal)	1	15ft.lb (20J)	10%	13mils (0.330mm)
	2	11.5ft.lb (16J)	10%	8mils (0.203mm)
	3	10ft.lb (14J)	10%	7mils (0.178mm)
0.25 Diameter (Transverse)	1	11ft.lb (15J)	10%	11mils (0.279mm)
	2	7ft.lb (9.5J)	10%	6mils (0.152mm)
	3	7ft.lb (9.5J)	10%	7mils (0.178mm)

Table 6. Failed shaft room temperature Charpy impact results

Temperature	Sample	Absorbed Energy ⁽¹⁾	Lateral Expansion
73°F (23°C)	1	221ft.lb (300J)	102mils (2.6mm)
	2	221ft.lb (300J)	102mils (2.6mm)
	3	221ft.lb (300J)	98mils (2.5mm)
14°F (-10°C)	1	164ft.lb (223J)	83mils (2.1mm)
	2	163ft.lb (221J)	83mils (2.1mm)
	3	162ft.lb (220J)	83mils (2.1mm)
-58°F (-50°C)	1	48ft.lb (65J)	32mils (0.8mm)
	2	57ft.lb (77J)	28mils (0.7mm)
	3	53ft.lb (72J)	28mils (0.7mm)

Table 7. Shaft forging supplier Charpy impact results (before machining and stress relief)



46TH **TURBOMACHINERY** & 33RD **PUMP SYMPOSIA**
HOUSTON, TEXAS | DECEMBER 11-14, 2017
GEORGE R. BROWN CONVENTION CENTER

Additionally, examination of the throttle sleeve showed evidence of thermal distortion/wear, see Figures 18 and 19. However, it could not be confirmed if the damage to the sleeve occurred before or after the shaft failure, though it appeared somewhat old. The tungsten carbide coating has chipped away due to the excessive temperature. One possible cause was filter media contamination of the sleeve/bushing. Operations had had trouble with the suction filters on the pump plugging and then blowing through.



Figure 18. breakdown of tungsten carbide coating on throttle sleeve



Figure 19. Close up of failed coating on throttle sleeve

Further testing of another large super duplex pump shaft revealed similar fracture toughness numbers. However, this shaft had been in operation for several years without any issues. While neither the O-ring groove or low fracture toughness alone should have caused the failure, it was accepted that the combination of both along with the possible distress of the sleeve contributed to the shaft failure. The operator and supplier wanted to make improvements where practical to mitigate future shaft failure incidents. The improvements implemented to address the failure included the following:

- Modify the throttle sleeve and shaft design so that the O-ring grooves are located in the sleeve only. This will eliminate the possibility of a stress riser in the groove initiating a crack in the shaft, see Figure 20.
- Modify the stress relieving procedure to improve the fracture toughness of the super duplex shaft forging.

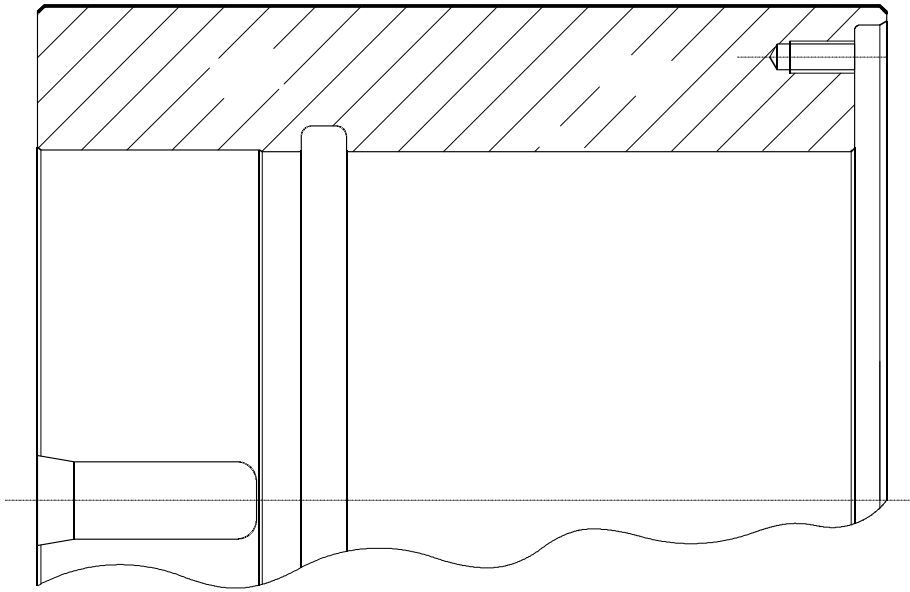


Figure 20. Sleeve modification with O-ring groove cut in sleeve only

After the shaft failure, the spare cartridge with 285 mm impellers was installed in the B pump casing. The pump operated normally for several months until operations personnel noticed an unusual noise and vibration when the B pump was in operation. A predictive maintenance technician was called to investigate the noise and discovered a unique situation. The pressure pulsation in the equalizing chamber / balance line was very high: appx 41-48 bard (600-700 psid), see Figure 21. The bushing/sleeve in Figure 14, reduces the pressure on the outboard end of the pump from approximately 276 to 19 bar (4000 to 280 psig). Because the pressure pulsation seemed unreasonably high, the pulsation was recorded in the same location on the A pump, see Figure 22. This confirmed that the pressure recording was correct. Because of the previous issue with the broken shaft, it was decided to pull the B pump cartridge and tear down the pump.

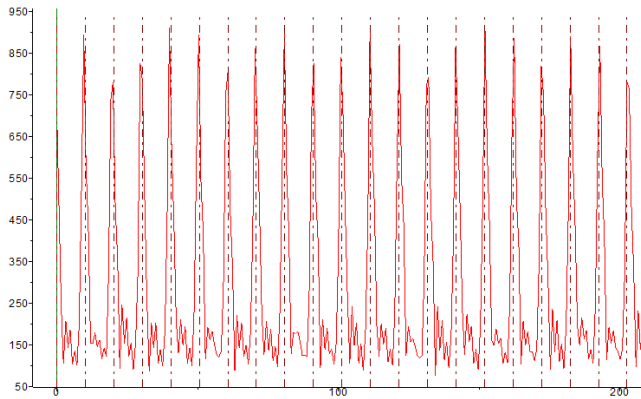


Figure 21. Dynamic pressure pulsation (psi) recorded on B pump balance line during operation (appx 150 to 850 psi)

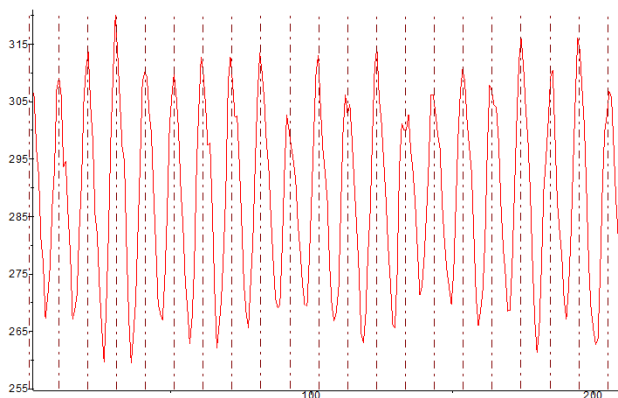


Figure 22. Dynamic pressure pulsation (psi) recorded on A pump balance line during operation (appx 265 to 315 psi)

Inspection of the pump didn't reveal a broken shaft as was found previously; however, the problem was found in the same location. Figure 23 is an enlarged view of the outboard bushing/sleeve shown in Figure 14 above. The sleeve has a relatively low interference fit to the shaft of appx 25 to 50 μm (0.001-0.002 in) and requires a pair of O-rings between it and the shaft to seal the almost 276 bard (4000 psid) of differential pressure. A shrink fit with higher interference to eliminate the need for o-rings was not selected by the OEM because this would have increased the sleeve thickness. The would have had increased shaft stresses since the sleeve acts like a piston with differential pressure. Because of the high differential, a set of split rings with a keeper ring secures the sleeve to the shaft axially. Inspection of



46TH TURBOMACHINERY & 33RD PUMP SYMPOSIA
HOUSTON, TEXAS | DECEMBER 11-14, 2017
GEORGE R. BROWN CONVENTION CENTER

the pump found that the inboard O-ring (left hand side of Figure 23) under the sleeve had been cut, probably during installation, see Figure 24. The split rings and the axial groove in the shaft showed evidence of fretting, see Figures 25 and 26. This indicates that the rings were being loaded axially in a cyclic manner. The failure of the inboard O-ring allowed high pressure water to migrate a significant length under the sleeve. This may have caused the sleeve to “bow” or “flap” on the shaft, causing the pressure pulsation in the balance chamber. The pump OEM used an FEA model to simulate the effect of the failed O-ring on the sleeve, see Figure 27. As a solution, the throttle sleeve design was modified again to reduce the possibility of damaging the O-ring on installation by increasing the chamfer on the inlet side in alignment with newer designs of the same pump type which were introduced in the meantime. Installation of the spare cartridge in the B pump lowered the pulsation to approximately 7 bard (200 psid), see Figure 28, but still higher than the A pump which had only 3.2 bard (50 psid). Both pumps have operated for the past 3 years with no more reliability issues. The pulsation on the balance chamber is still routinely recorded and has not increased.

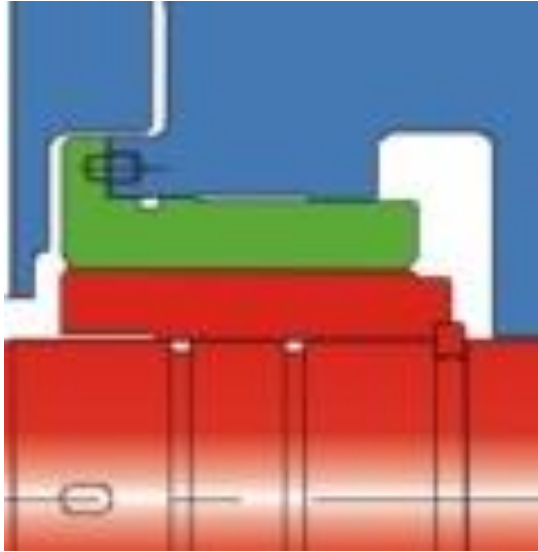


Figure 23. Detail of throttle bushing (green) and sleeve (red) on shaft (Sulzer)



Figure 24. Inboard(LHS) and outboard(RHS) O-rings from throttle sleeve

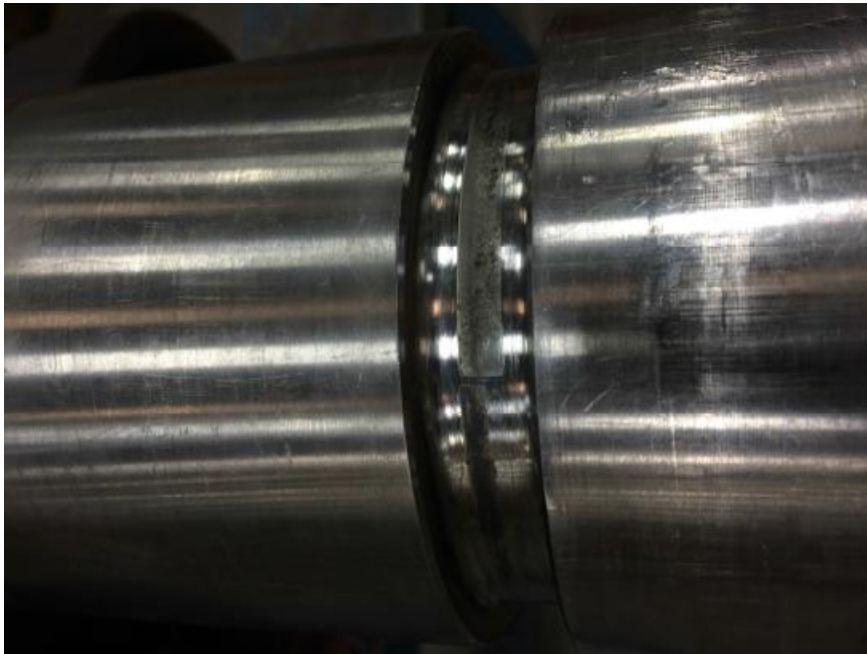


Figure 25. Shaft groove for split rings showing fretting from vibration



Figure 26. Fretting on split rings, evidence of vibration

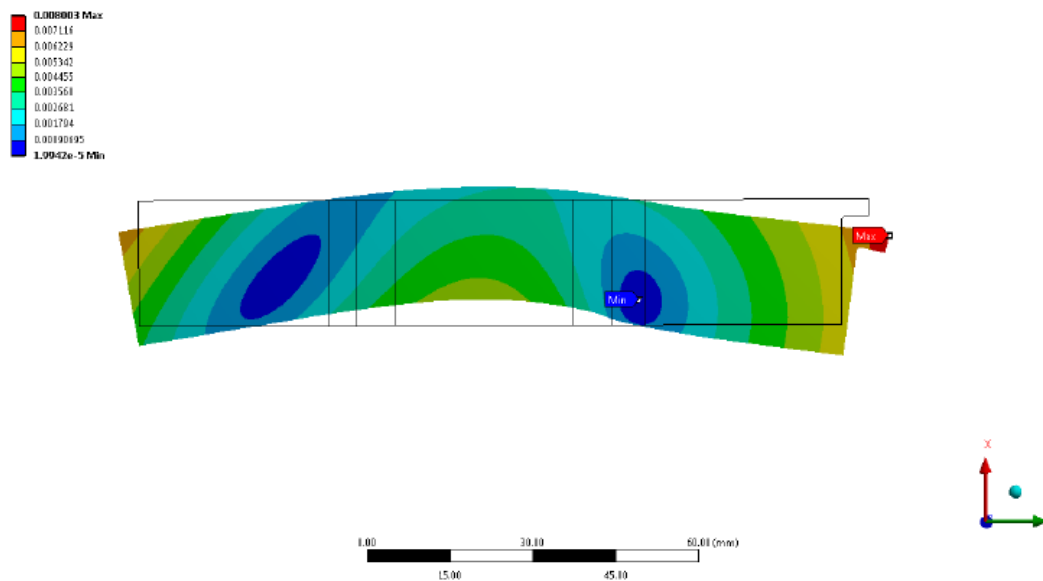


Figure 27. FEA model of sleeve with failed inboard O-ring, showing exaggerated deformation(Sulzer)

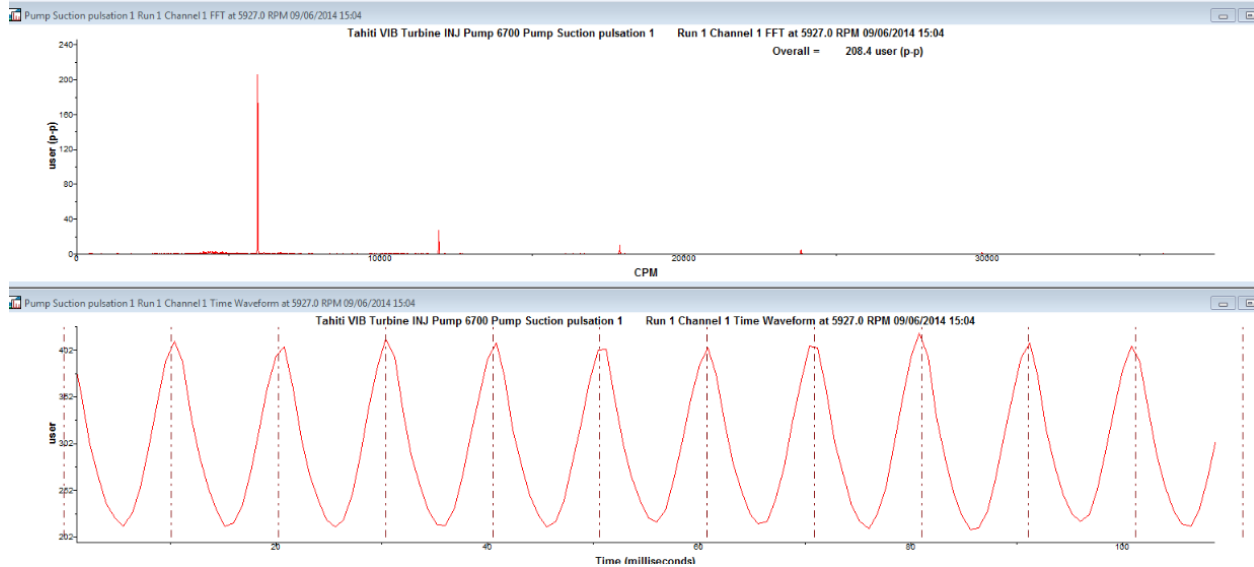


Figure 28. Measured dynamic pulsation (psi) on B pump after replacement cartridge was re-installed appx 14 bard (185 psid), from measured pressure in range of 15 to 28 bar (220 to 405 psi)

CONCLUSIONS

A large part of the technical qualification of the pump concentrated on evaluating the impeller natural frequencies and the predicted fatigue life. While the measured pulsation at the 1st stage impeller during the FAT was a significant concern, the pumps have operated for approximately 5 years without any impeller failures or cracks. However, the issues with the failed shaft and high pressure pulsation on the balance chamber have proven to be very challenging. These issues emphasize the vast difference between field proven technology and shop tested technology as well as the need for detailed qualification of new technology.



46TH **TURBOMACHINERY** & 33RD **PUMP SYMPOSIA**
HOUSTON, TEXAS | DECEMBER 11-14, 2017
GEORGE R. BROWN CONVENTION CENTER

REFERENCES

- [1] Meuter, Lienau, Schachenmann, Germaine, McDonald: “Thunder Horse Injection pump”, 2003, Proceedings of the Twentieth International Pump Users Symposium, Turbomachinery Laboratory, Texas, US.
- [2] Dr. S. Berten: “Hydrodynamics of High Specific Power Pumps for Off-Design Operating Conditions”, 2010, EPFL, Lausanne, Switzerland.
- [3] S. Berten, K. Kieselbach, P. Dupont, S. Hentschel: “Experimental and Numerical Analysis of Pressure Pulsations and Mechanical Deformations in a Centrifugal Pump Impeller”, Sulzer Pumps, S. Hentschel, Karlsruher Institut für Technologie (KIT), Proceedings of ASME – JSME Joint Fluids Engrg Conference July 2011 – AJK2011-06057